CAFs-derived HSPA1A promotes gastric cancer growth and affects chemotherapy by interacting with SEMG1 and regulating glycolysis

Jia XU
xujia@renji.com
Shanghai Jiao Tong University
Tian-Shang Bao
Shanghai Jiao Tong University
Fei Wang
Shanghai Jiao Tong University
Guang-Hong Su
Shanghai Jiao Tong University
Rui Lu
Shanghai Jiao Tong University
Ting-Hong Wei
thwei1103@126.com
Hui Li
Shanghai Jiao Tong University
Shuang-Qin Yi
Tokyo Metropolitan University, Japan https://orcid.org/0000-0002-9946-7895
Shu-Heng Jiang
Shanghai Cancer Institute, Ren Ji Hospital, School of Medicine, Shanghai Jiao Tong University
https://orcid.org/0000-0001-8516-6234
Qing Li
Shanghai Cancer Institute, Ren Ji Hospital, School of Medicine, Shanghai Jiao Tong University
https://orcid.org/0000-0002-3579-5494
Li-Peng Hu
State Key Laboratory of Oncogenes and Related Genes, Shanghai Cancer Institute, Ren Ji Hospital, School of Medicine, Shanghai Jiao Tong University https://orcid.org/0000-0002-5941-3825
Jun Li
Shanghai Jiao Tong University https://orcid.org/0000-0003-0423-3381
Hui Cao

Shanghai Jiao Tong University

Article

Keywords: Gastric cancer(GC), cancer-associated fibroblast (CAF), HSPA1A, SEMG1, glycolysis

Posted Date: February 12th, 2026

DOI: https://doi.org/10.21203/rs.3.rs-8696092/v1

Additional Declarations: (Not answered)

CAFs-derived HSPA1A promotes gastric cancer growth and affects chemotherapy by interacting with SEMG1 and regulating glycolysis

Tian-Shang Bao[1,*], Fei Wang[1,*], Guang-Hong Su[2,*], Rui Lu[2,*], Ting-Hong Wei[2,*], Hui Li[2], Shuang-Qin Yi[3], Qing Li[2,#], Li-Peng Hu[2,#], Jun Li[2,#], Hui Cao[1,#], Jia Xu[1,#]

[1]Department of Gastrointestinal Surgery, Renji Hospital, School of Medicine, Shanghai Jiao Tong University, Shanghai, China.

[2]State Key Laboratory of Systems Medicine for Cancer, Shanghai Cancer Institute, Ren Ji Hospital, School of Medicine, Shanghai Jiao Tong University, Shanghai, China.

[3]Department of Frontier Health Sciences, Graduate School of Human Health Sciences, Tokyo Metropolitan University, Japan.

[*]Tian-Shang Bao, Fei Wang, Guang-Hong Su, Rui Lu and Ting-Hong Wei contributed equally to this work.

[*]Correspondence to: Jia Xu, Department of General Surgery, Renji Hospital, School of Medicine, Shanghai Jiao Tong University, 160 Pujian Road, Shanghai 200127, China.

Hui Cao, Department of General Surgery, Renji Hospital, School of Medicine, Shanghai Jiao Tong University, 160 Pujian Road, Shanghai 200127, China.

Jun Li, State Key Laboratory of Oncogenes and Related Genes, Shanghai Cancer Institute, Ren Ji Hospital, School of Medicine, Shanghai Jiao Tong University, 800 Dongchuan Road, Shanghai 200240, China.

Li-Peng Hu, State Key Laboratory of Oncogenes and Related Genes, Shanghai Cancer Institute, Ren Ji Hospital, School of Medicine, Shanghai Jiao Tong University, 800 Dongchuan Road,

Shanghai 200240, China.

Qing Li, State Key Laboratory of Oncogenes and Related Genes, Shanghai Cancer Institute, Ren Ji Hospital, School of Medicine, Shanghai Jiao Tong University, 800 Dongchuan Road, Shanghai 200240, China.

E-mail addresses: xujia201800@126.com (J. Xu), caohuishcn@hotmial.com (H. Cao), junli@shsci.org (J. Li), lphu@shsci.org (L.P. Hu), 13851601478@163.com (Q. Li).

Abstract

Gastric cancer (GC) progression and drug resistance are strongly influenced by the tumor microenvironment, especially cancer-associated fibroblasts (CAFs). This study aimed to clarify the role of CAF-derived HSPA1A in GC growth and chemosensitivity and to explore the underlying mechanism.

HSPA1A expression and clinical relevance were evaluated using the GEO dataset (GSE163558) and immunohistochemistry (IHC) on 168 cases of GC tissue microarray. Immunofluorescence (IF) with the CAF marker FAP were used to identify the cellular source of HSPA1A. Functional effects of HSPA1A were examined in CAF–GC cell co-culture systems, tumor sphere assays, patient-derived organoids, and a subcutaneous xenograft model. RNA-sequencing (RNA-seq), co-immunoprecipitation (co-IP), Western blotting, and Seahorse glycolysis assays were used to identify HSPA1A-interacting proteins and to assess glycolytic activity.

Through the above experiments, we found that HSPA1A was upregulated in GC tissues and associated with advanced T stage and poor prognosis, and was predominantly expressed in CAFs. Silencing HSPA1A in CAFs reduced GC cell proliferation, migration, and sphere formation, inhibited organoid growth, and enhanced sensitivity to 5-fluorouracil(5-FU), with similar effect on paclitaxel (PTX). In vivo, HSPA1A blockade suppressed xenograft growth and potentiated chemotherapy. Mechanistically, SEMG1 was identified as a binding partner of HSPA1A.

So we concluded that targeting the HSPA1A–SEMG1 axis decreased expression of glycolysis-related enzymes, reduced glycolytic flux, and synergistically impaired GC cell growth. CAFs-

derived HSPA1A promotes GC progression and 5-FU resistance by interacting with SEMG1 and enhancing glycolysis in tumor cells. The HSPA1A–SEMG1 axis represents a potential therapeutic target to inhibit GC growth and improve chemosensitivity.

Keywords Gastric cancer(GC), cancer-associated fibroblast (CAF), HSPA1A, SEMG1, glycolysis

Introduction

As one of the most Prevalent malignant tumor of the digestive system[1], gastric cancer (GC) remains a major global health burden with high incidence and mortality[2][3], and most patients are diagnosed at advanced stages when therapeutic resistance is common[4][5][6]. Increasing evidence has demonstrated that the tumor microenvironment (TME) plays a critical role in GC progression and drug response[7][8][9]. Among stromal components, cancer-associated fibroblasts (CAFs) are the predominant non-malignant population within GC tissues and actively support tumor growth, invasion, and immune evasion[9][11][12]. Targeting CAF-mediated tumor–stromal interactions has therefore emerged as a promising strategy to improve treatment efficacy in GC[13][14].

Heat shock protein family members are frequently upregulated in malignancies and contribute to tumor survival under stress conditions[15][16][17]. HSPA1A, a major inducible isoform of the HSP70 family, acts as an ATP-dependent molecular chaperone that prevents protein misfolding, protects cells from apoptosis, and promotes metabolic adaptation[18][19][20]. Elevated HSPA1A expression has been linked to unfavorable prognosis and treatment resistance in multiple cancers[21]. However, current research has primarily focused on tumor-cell-intrinsic HSPA1A, whereas its role in CAFs and the way it regulates GC cells remains largely unexplored.

Metabolic reprogramming, especially enhanced glycolysis, is a hallmark of GC progression and closely associated with chemoresistance, including resistance to 5-fluorouracil

(5-FU)[22][23]. SEMG1, a cancer-testis antigen aberrantly expressed in several tumor types, has been implicated in promoting tumor cell proliferation and energy metabolism[24][25]. Nonetheless, whether SEMG1 function is controlled by signals originating from CAFs is unknown.

Here, we identify HSPA1A as a CAF-derived factor highly upregulated in GC tissues and associated with aggressive clinicopathological features. We further show that CAF-derived HSPA1A directly interacts with SEMG1 in GC cells to activate glycolytic signaling, thereby promoting tumor growth and weakening the response to chemotherapy. These findings reveal the previously unrecognized CAF-HSPA1A–SEMG1 axis as a crucial regulator of GC metabolic adaptation and provide a potential therapeutic target to enhance chemosensitivity.

Method

Regent

The primary antibodies used in the experiment include HSPA1A (Proteintech, 10995-1-AP, China), PDPN (Proteintech, 116291-1-AP, China), S100A4 (Proteintech, 16105-1-AP, China), GAPDH (Proteintech, 60004-1-Ig, China), FAP (Immunoway, PT0578R, China), SEMG1 (Immunoway, YT-7170, China), LADH(Uping Biotech, YP-Ab-07877, China), PKM2 (Uping Biotech, YP-Ab-02757, China).

Clinical samples

This study was approved by the Ethics Committee of Renji Hospital, School of Medicine, Shanghai Jiao Tong University, and informed consent was obtained from all participants. The tissue samples of GC patients were obtained from the Department of Gastrointestinal Surgery, Renji Hospital, School of Medicine, Shanghai Jiao Tong University. The tissue microarray included GC lesion tissues and adjacent normal gastric tissues, and a total of 168 cases of GC tissues from December 2017 to September 2022 were selected. Approval letter of Shanghai Jiaotong University School of Medicine, Renji Hospital Ethics Committee is KY2024-046-C.

Immunohistochemistry staining (IHC)

Perform routine hematoxylin and eosin (HE) staining[26]. Immunohistochemical staining was performed on tumor microarrays (TMAs) and paraffin sections. Briefly, tissues were fixed in formalin, embedded in paraffin, and then cut into 5-μm-thick sections. The sections were dewaxed in xylene and rehydrated in graded ethanol for histopathological evaluation. Antigen retrieval was performed by placing the sections in a high-temperature microwave oven for 5 minutes, repeating 2 - 3 times. After treatment with 0.3% hydrogen peroxide/phosphate-buffered saline for 30 minutes, the sections were blocked with 10% BSA at room temperature for 1 hour. Then, the sections were incubated overnight at 4 °C with primary antibodies against HSPA1A (1:2000, Proteintech, 10995-1-AP), SEMG1 (1:2000, Immunoway , YT-7170), FAP(1:2000, Immuoway, PT0578R) diluted to the optimal concentration. Then, the sections were incubated with HRP-conjugated mouse or rabbit secondary antibodies at room temperature for 1 hour. The sections were then incubated with DAB substrate solution (No. S210242, Thermo Scientific, USA) and counterstained with hematoxylin. All sections were observed and photographed using a Carl Zeiss microscope[27].

Immunofluorescence (IF)

Cells cultured in ibidi 8-well chambers were washed with PBS, fixed with 4% paraformaldehyde for 10 min at room temperature, washed three times with PBS (5 min each), and blocked with 5% BSA in PBS for 1 h. PDPN+FAP (no permeabilization). Cells were incubated overnight at 4 °C with Syrian hamster anti-mouse PDPN (clone 8.1.1, 1:400, Sigma-Aldrich/Merck Millipore, MABT1512) and rabbit anti-FAP (1:400, Proteintech, 11779-1-AP) diluted in blocking buffer. After three PBS washes, cells were incubated for 1 h at room temperature in the dark with Alexa Fluor 594–conjugated goat anti–Syrian hamster IgG (H+L) (1:500, Jackson ImmunoResearch, 107-585-142) and Alexa Fluor 488–conjugated donkey anti-rabbit IgG (H+L) (1:500, Jackson ImmunoResearch, 711-545-152). Cells were washed and counterstained with DAPI for 10 min.

PDPN+S100A4 (sequential staining with permeabilization). To preserve membrane PDPN staining while enabling intracellular S100A4 detection, PDPN was stained prior to permeabilization. Cells were first incubated overnight at 4 °C with Syrian hamster anti-mouse PDPN (clone 8.1.1, 1:400, Sigma-Aldrich/Merck Millipore, MABT1512), washed, and

incubated with Alexa Fluor 594–conjugated goat anti–Syrian hamster IgG (H+L) (1:500, Jackson ImmunoResearch, 107-585-142) for 1 h at room temperature in the dark. Cells were then post-fixed with 4% paraformaldehyde for 5 min, washed, permeabilized with 0.1% Triton X-100 in PBS for 10 min, and re-blocked with 5% BSA for 30 min. Subsequently, cells were incubated overnight at 4 °C with rabbit anti-S100A4 (1:400, Proteintech, 16105-1-AP), washed, and incubated with Alexa Fluor 488–conjugated donkey anti-rabbit IgG (H+L) (1:500, Jackson ImmunoResearch, 711-545-152) for 1 h at room temperature in the dark. After PBS washes, nuclei were counterstained with DAPI for 10 min, washed, and samples were imaged using a Leica SP8 confocal microscope .

RNA Scope

Tissue sections in 5-μm thickness were deparaffinized in xylene, followed by dehydration in an ethanol series. Tissue sections were then incubated in citrate buffer (10 nmol/L, pH 6) maintained at a boiling temperature (100°C to 103°C) using a hot plate for 15 minutes, rinsed in deionized water, and immediately treated with10 μg/mL protease (Sigma-Aldrich, St. Louis, MO) at 40°C for 30 minutes in a HybEZ hybridization oven (Advanced Cell Diagnostics, Hayward, CA). Hybridization with target probes, preamplifier, amplifier, and label probe and chromogenic detection were as described above for cultured cells. A wide range of assay conditions were explored to optimize for FFPE samples prepared and fixed according to American Society of Clinical Oncology/College of American Pathologists (ASCO/CAP) guidelines14 (10% neutral buffered formalin for 6 to 72 hours at room temperature), including pretreatment conditions such as citrate buffer temperature, pH, incubation time, and protease concentrations[28].

Cell culture

Human GC cell lines AGS, HGC27, MKN28, MKN45, and KATO III were purchased from the American Type Culture Collection. Primary gastric fibroblasts (HUM - iCell - d006) were purchased from Shanghai Lan rong Biotechnology Co., Ltd. GC cell lines KATO III, SNU - 16 and gastric epithelial cell line GES - 1 were purchased from the Center for Excellence in Molecular Cell Science, Chinese Academy of Sciences. The GC cells were cultured in RPMI - 1640 medium (Gibco, New York, USA) supplemented with 10% fetal bovine serum (Gibco,

New York, USA) and 1% antibiotics (streptomycin and penicillin, Sigma - Aldrich, St. Louis, USA) in a humidified incubator at 37 °C with 5% CO2. The gastric fibroblasts were cultured in Special culture medium for human primary gastric fibroblasts (Shanghai Lan rong Biotech, China) supplemented with primary fibroblast culture additives, 10% fetal bovine serum (Gibco, New York, USA) and 1% antibiotics (streptomycin and penicillin, Sigma - Aldrich, St. Louis, USA) in a humidified incubator at 37 °C with 5% CO2.

Cell co-culture

Co-culture experiments were performed in Tissue Culture Transwell Plates (0.4 μm pore size, Corning, China). GC cell lines (2*10^4/well) were cultured in the bottom chamber, CAF were placed in the upper chamber[30].

Quantitative Real-time PCR

Total RNA was extracted using Trizol (9109, Takara, Japan) and reverse transcribed using the Prime Script RT-PCR Kit (Takara, #RR600A) according to the manufacturer's instructions. Quantitative real-time PCR assays were performed using SYBR Premix 2x Taq (Takara, Japan) on VIIA ™ 7 (Applied Biosystems ™, USA) under the recommended thermal cycling settings: an initial cycle at 95 °C for 15 minutes, followed by 40 cycles of 15 seconds at 95 °C and 30 seconds at 60 °C. Relative mRNA expression was calculated according to the 2(-ΔΔCt) method.

HSPA1A-Forward Primer:	AGCTGGAGCAGGTGTGTAAC
HSPA1A-Reverse Primer:	CAGCAATCTTGGAAAGGCCC
GAPDH-Forward Primer:	AATGGGCAGCCGTTAGGAAA
GAPDH-Reverse Primer:	GCCCAATACGACCAAATCAGAG
SEMG1-Forward Primer:	TGGATCTCATGGGGGATTGG
SEMG1-Reverse Primer:	TGAAGGCGCTTCAGGTTAGG
PKM2-Forward Primer:	GTGGCTCGTGGTGATCTAGG
PKM2-Reverse Primer:	AGCCTCACGAGCTATCAGGT
LDHA-Forward Primer:	CCGACGTGCATTCCCGATT
LDHA-Reverse Primer:	AGGTCAAGATATCCACTTTGCCA

Lentivirus production and cell transduction

According to the standard protocol, virus packaging was performed in 293T cells after co-transfection of the pEZ-lv105 vector (Gene Coplant, Shanghai, China) using Lipofectamine 2000 (Invitrogen, Carlsbad, CA). Lentiviruses were harvested 48 and 72 hours after transfection. Cells were infected with 1 × 10^6 recombinant lentiviral transduction units in the presence of 5 μg/ml polybrene (Sigma, #H9268, #P7130). After 48 hours of infection, the cells were incubated with puromycin (Gibco, #A1113802) at a dose of 1.0 μg/ml for more than 7 days until no more obvious cell death was observed. Puromycin-resistant cells were obtained, and the knockdown or overexpression efficiency was verified by Western blotting.

Western Blotting

Collect the lysates of protein samples in RIPA lysis buffer (YOCHE., YSD 0100) on ice for at least 20 min, and centrifuge at 12 000 × g for 20 min at 4 °C. Dilute with 5 × loading buffer and boil for 10 min. Separate the proteins by SDS-PAGE and transfer them to a nitrocellulose membrane. Subsequently, wash the membrane with TBST and block it with a 5% non-fat milk solution diluted in TBST at room temperature for 1 hour. Then incubate the membrane with the primary antibody overnight at 4 °C. Then incubate them with the HRP-conjugated secondary antibody at room temperature for 1 hour. Finally, visualize the bands with ECL reagent (ShareBio, SB-WB001).

Cell Counting Kit-8 (CCK-8) viability assay

To measure cell proliferation, the specified cells were seeded in triplicate in 96-well plates at a medium density (10^4 cells/ml). Next, 100ul CAF supernatant or 100ul si-HSPA1A CAF supernatant culture medium containing 10% Cell Counting Kit-8 (CCK-8) reagent (Dojindo, Japan) was added to each well, and the samples were incubated at 37 °C for 1 hour, continuously for 4 days. Then, the absorbance was measured at a wavelength of 450 nm using a multi-functional microplate reader.

Organoid culture

The clinically obtained tumor samples were frozen and transferred to the laboratory. Briefly, the dissected tumors were minced and transferred to a 50 ml centrifuge tube containing a digestion mixture composed of Ad-DMEM/F-12 medium (Gibco, USA) and 1 mg/ml collagenase IV (Sigma, USA), and incubated at 37°C for 40 minutes. The isolated organoids were mixed with 5 μL of Matrigel (Costar, USA) and seeded in a 96-well plate (Costar, USA). The medium contained Ad-DMEM/F-12 and B27 supplement (1×), nicotinamide (10 mM), N-acetyl-l-cysteine (1.25 mM), EGF (5 ng/ml), A83-01 (500 nM), SB202190 (10 μM), Y-27632 (10 μM), Noggin (100 ng/mL), R-Spondin 3 (250 ng/ml), FGF2 (5 ng/ml), FGF 10 (10 ng/ml), penicillin/streptomycin (1×), and glutamine (1×). Supplemented medium (100 μL) was added to each well, and the organoids were maintained in a humidified atmosphere of 5% CO2 at 37°C[31].

Construction of subcutaneous tumor model in mice

For the subcutaneous xenograft model of AGS cells, nude mice at 4 weeks of age were used. Briefly, 2×10^6 AGS cells were suspended in a total of 100 μL of PBS and Matrigel, and subcutaneously implanted into the inguinal region of the mice. When the tumor volume reached approximately 50 mm^3, the mice were randomly divided into two groups. 50 ul PBS and 50ul HSPA1A Antibody - BSA Free (1:200, NBP1-77456; Novus Bio, Littleton, CO, USA) were injected respectively once every other day. One week later each group were randomly divided into 4 groups (n = 3), and 100 μL of 5 - FU and 100 μL of PTX were injected peritumorally once every other day.

Co-immunoprecipitation assay

Co-immunoprecipitation (Co-IP) experiment was performed using a universal toolkit (KTD104, Abbkine, China) containing protein A/G magnetic beads. Firstly, cell protein was extracted from the nondenaturing lysis buffer and then quantified using the bicinchoninic acid (BCA) assay kit (KTD3001, Abbkine, China). Next, cell lysates and magnetic beads were precleared to remove nonspecific binding, and the supernatant was obtained from magnetic separation rack. Then, 1 μg HSPA1A antibody or SEMG1 antiboday was mixed with 20 μL magnetic beads and rabbit IgG negative control was set at the same time. Finally, 200 μg supernatant was

added to the above two groups and incubated at 4°C overnight. The next day, this immune complex was eluted by denatured methods for sodium dodecyl sulfate-polyacrylamide gel electrophoresis (SDS-PAGE) and western blotting analysis[32].

Wound-healing assay

Cells were seeded in a six-well plate and grown to 80% confluence. A wound was carefully scrapped with a sterilized pipette tip in the middle of the cell monolayer. Photomicrographs were taken every 12 h during incubation. The wound width in the microscopic pictures were measured by ImageJ software version 1.37 (National Institutes of Health) at different time points. The percentage of wound healing was calculated from the initial wound width at 0 h.

Measurement of glycolytic rate

The glycolytic rate was determined using the Seahorse XF Glycolysis Rate Assay Kit (Alicelligent, China, ALS22023) following the manufacturer's instructions. Briefly, XFe 96-well cell culture microplates were pre-coated with Cell-Tak (Corning, China). On the day of the assay, cells were resuspended in assay medium supplemented with 1 mM pyruvate, 2 mM glutamine, and 10 mM glucose, and then seeded into the pre-coated plates. Cells were sequentially treated with 0.5 μM rotenone/antimycin A (Rot/AA) and 50 mM 2-DG. The assay was conducted using the Agilent Seahorse XFe 24 Analyzer, and data were acquired and analyzed using Wave Desktop software. The glycolytic rate was calculated based on extracellular acidification rate (ECAR) measurements, and the results were graphically represented for comparative analysis.

Tumor sphere formation assay

The effect of the HSPA1A - SEMG1 axis on the proliferation of GC was verified through the tumor sphere formation assay. 5000 digested cells were seeded into the Transwell chambers of a 12 - well plate containing 1640 medium with Matrigel and 10% FBS. The lower layer was DMEM medium containing 10% FBS. Each well was examined under an optical microscope every 3 days. After 7 days, the number of tumor spheres larger than 100 μm was counted. Images of the tumor spheres were taken with a microscope, and the size of the tumors was measured using ImageJ software.

Statistical analysis

If there are no special instructions, data were presented as the means ± standard errors of the mean (SEMs). The statistical analyses of the characteristics of GC were done using SPSS 27.0 for Windows (IBM). Other statistical analyses were performed using GraphPad Prism 10 for Windows. One-way ANOVA or two-tailed Student's t test was used for comparisons between groups. Values of $P < 0.05$ were considered statistically significant.

Result

CAF-derived HSPA1A is upregulated in GC and correlates with poor prognosis

Analysis of the single-cell RNA-sequencing dataset GSE163558 revealed that HSPA1A was markedly upregulated in CAFs compared with other stromal and immune cell types in GC tissues (**Fig. 1A-B**). Differential expression analysis further confirmed elevated HSPA1A levels in CAFs from GC tissues compared with paracancerous (PC) tissues or metastatic lymph nodes (**Fig. 1C–D**).

To validate these findings in clinical samples, immunohistochemistry on a tissue microarray containing 168 paired GC and adjacent tissues demonstrated that HSPA1A expression was significantly higher in tumor tissues, both in epithelial regions and surrounding stroma (**Fig. 1E–F**). Increased stromal HSPA1A expression was positively associated with advanced T stage (T3/T4), indicating a link to local tumor aggressiveness (**Fig. 1F**).

Survival analysis using the KM-Plot database showed that patients with high HSPA1A expression had significantly worse overall survival than those with low expression, suggesting that HSPA1A may serve as a negative prognostic biomarker (**Fig. 1G**)[29].

To determine the cellular origin of HSPA1A, immunofluorescence co-staining revealed strong spatial colocalization between HSPA1A and the CAF marker FAP in the tumor stroma (**Fig. 1H**). RNA scope analysis further confirmed that HSPA1A transcripts were predominantly restricted to fibroblast-rich regions, rather than tumor epithelial compartments. An apparent increase in HSPA1A signals was observed across representative specimens from carcinoma in

situ to early - stage GC and then to advanced - stage GC. (**Fig. 1I**).

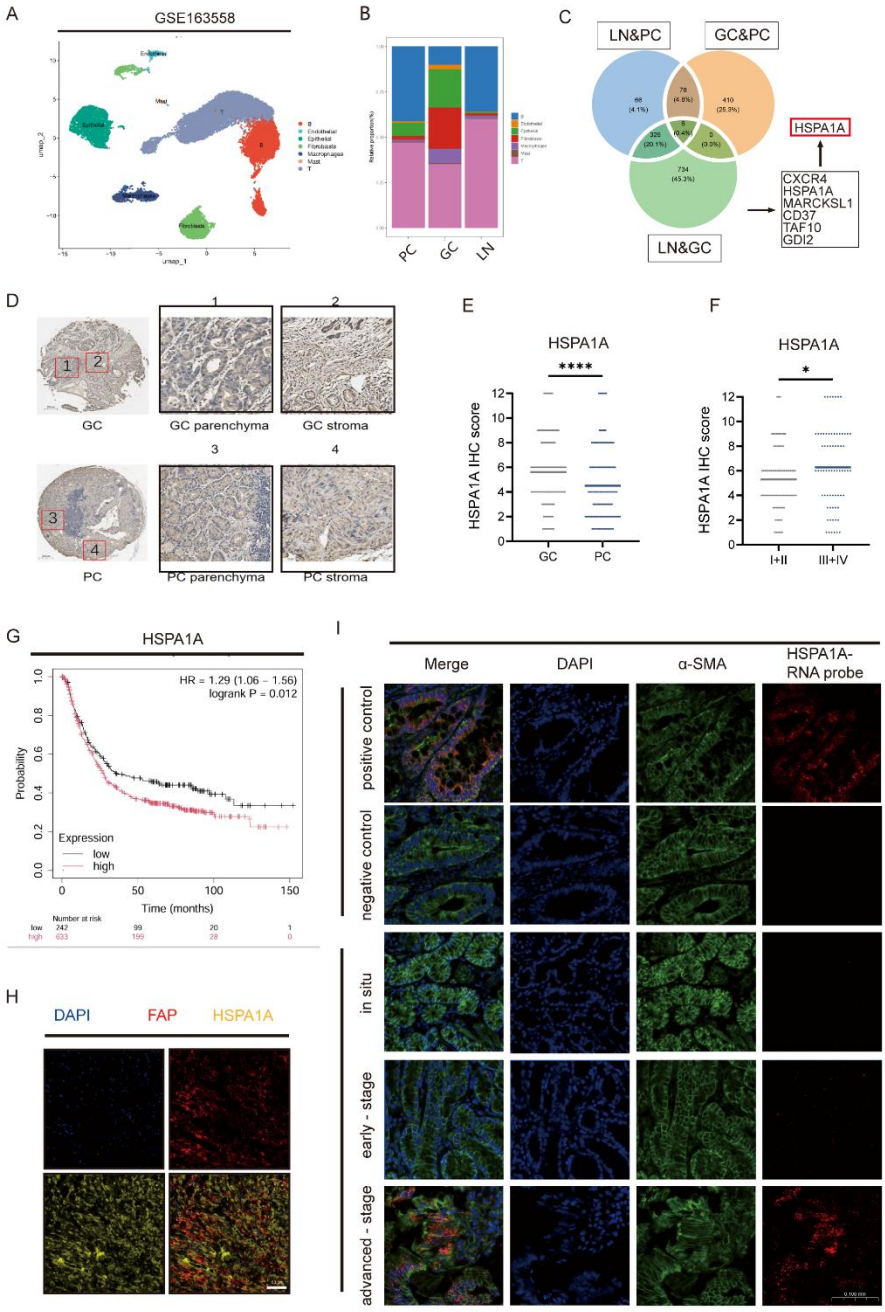

Figure 1. HSPA1A is significantly up-related in GC associated fibroblasts and closely related with prognosis.

A. UMAP plot of the single-cell dataset GSE163558 for GC;

B. Distribution proportions of sub - populations such as B cells, endothelial cells, epithelial cells, and fibroblasts in the dataset among the PC tissues, GC tissues, and lymph node (LN)

tissues of GC;

C. Genes upregulated in CAFs in GC and PC tissues, GC and LN tissues, and PC and LN tissues, including HSPA1A;

D. Analysis of IHC staining results of the parenchyma and stroma in GC and PC tissues;

E. Statistical analysis of HSPA1A in GC and PC tissues in 168 patients;

F. Statistical analysis of HSPA1A in advanced T stage (Ⅰ + Ⅱ -T1/T2, Ⅲ+Ⅳ -T3/T4) of GC tissues in 168 patients;

G. Kaplan–Meier analysis of overall survival stratified by HSPA1A expression;

H. IF Staining of HSPA1A and FAP in GC patients;

I. RNA scope validation of HSPA1A transcripts in clinical samples.

*P<0.05; ****P<0.0001.

Together, these data indicate that HSPA1A is mainly derived from CAFs in GC tissues and that CAF-associated HSPA1A expression correlates with tumor progression and poor patient prognosis.

Knocking down CAF-derived HSPA1A impairs GC cell growth and motility in vitro

To investigate the functional role of CAF-derived HSPA1A, normal gastric fibroblasts (FRCs) were induced into CAF-like cells through co-culture with GC cell lines. These induced CAFs showed strong expression of CAF markers FAP and S100A4 (**Fig. 2A**). Silencing HSPA1A in CAFs using siRNA markedly reduced HSPA1A levels in both cell lysates and secreted supernatants, as confirmed by Western blotting and qPCR (**Fig. 2B–C**).

Functionally, CAFs significantly promoted the proliferation of AGS and HGC27 cells, whereas HSPA1A-deficient CAFs failed to support tumor cell proliferation, resulting in significantly reduced cell viability in CCK-8 assays (**Fig. 2D**). Likewise, wound-healing assays showed that CAF-derived HSPA1A enhances GC cell migration, and loss of HSPA1A in CAFs markedly impaired the wound-closure ability of AGS and HGC27 cells (**Fig. 2E–F**).

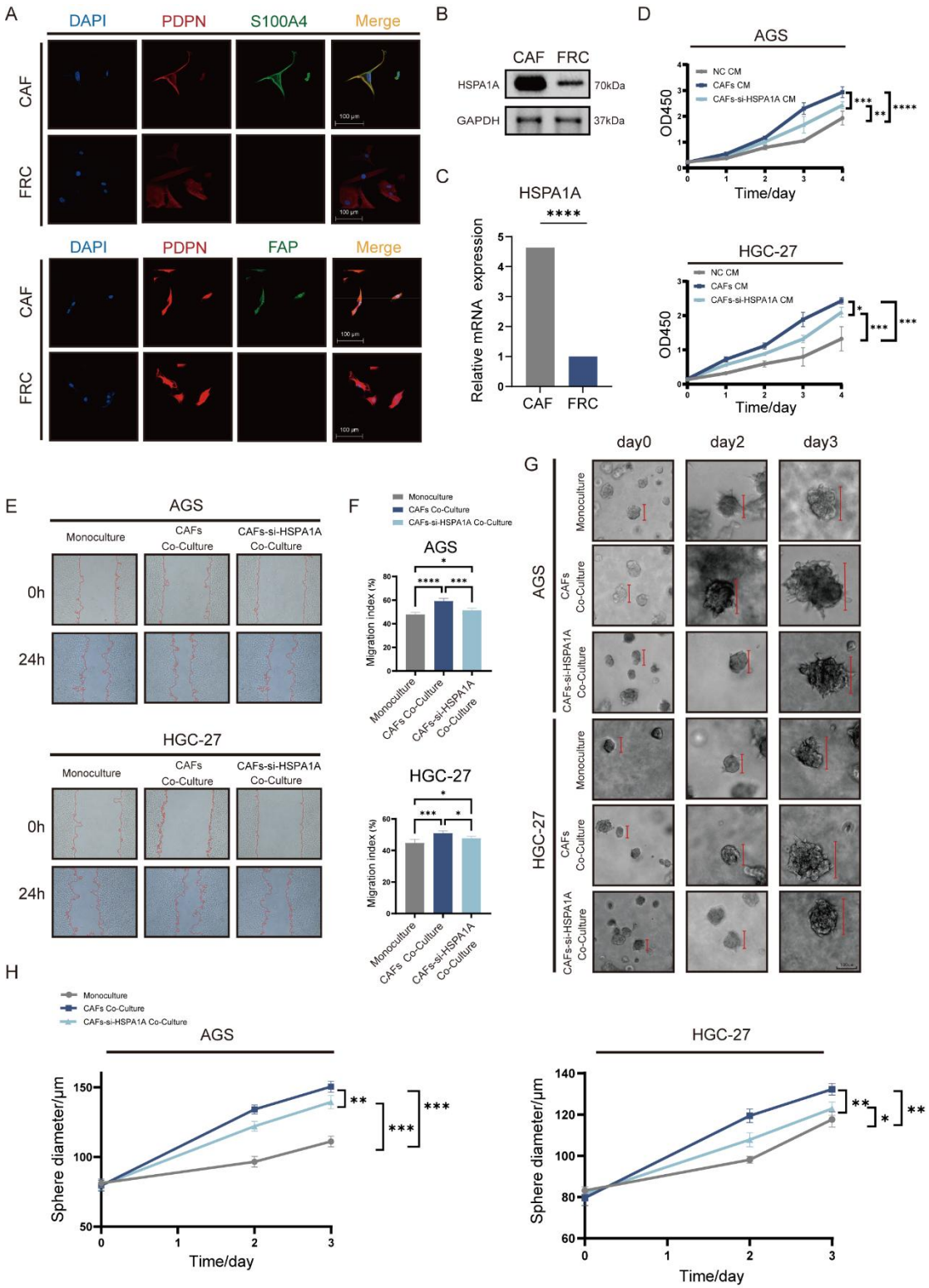

Figure 2. Knockdown of HSPA1A in CAFs suppresses GC cell growth and migration.

A. IF detection of CAF - related markers. PDPN: red, FAP: green, S - 100A4: green, DAPI: blue;

B and C. Western blotting and qPCR verification of the expression difference of HSPA1A in normal gastric fibroblasts and CAFs;

D. CCK8 assay to determine the growth ability of AGS and HGC27 after knocking down

HSPA1A in CAFs;
E and F. Cell scratch assay to measure the migration ability of AGS cells and HGC27 cells in the co - culture system;
G and H. Measurement of the sphere-forming ability and sphere diameter of AGS and HGC27 in the co-culture system.
*P<0.05; **P<0.01; ***P<0.001; ****P<0.0001.

Additionally, CAFs increased tumor-sphere numbers and diameters, while HSPA1A knockdown substantially decreased sphere-forming capacity in co-culture conditions **(Fig. 2G-H)**, indicating that CAF-derived HSPA1A supports stem-like features of GC cells.

CAF-derived HSPA1A promotes the expansion of GC organoids

To further validate the tumor-promoting function of CAF-derived HSPA1A in a more physiologically relevant 3D model, we established a co-culture system using patient-derived GC organoids and CAFs (**Fig. 3A**). Compared with organoids cultured alone, co-culture with CAFs markedly enhanced organoid growth, reflected by increased organoid diameter and structural complexity (**Fig. 3B–C**).

Importantly, siRNA-mediated knockdown of HSPA1A in CAFs significantly attenuated this CAF-induced organoid expansion, leading to smaller organoids (**Fig. 3B–C**). Likewise, treatment with a neutralizing HSPA1A-blocking antibody in CAFs produced a similar reduction in organoid growth (**Fig. 3B–C**), confirming that secreted HSPA1A from CAFs is required for stromal support of tumor growth.

Notably, silencing or antibody blockade of HSPA1A in organoids alone did not significantly affect organoid size (**Fig. 3C**), suggesting that HSPA1A primarily functions as a stromal-derived rather than tumor-intrinsic factor in this context.

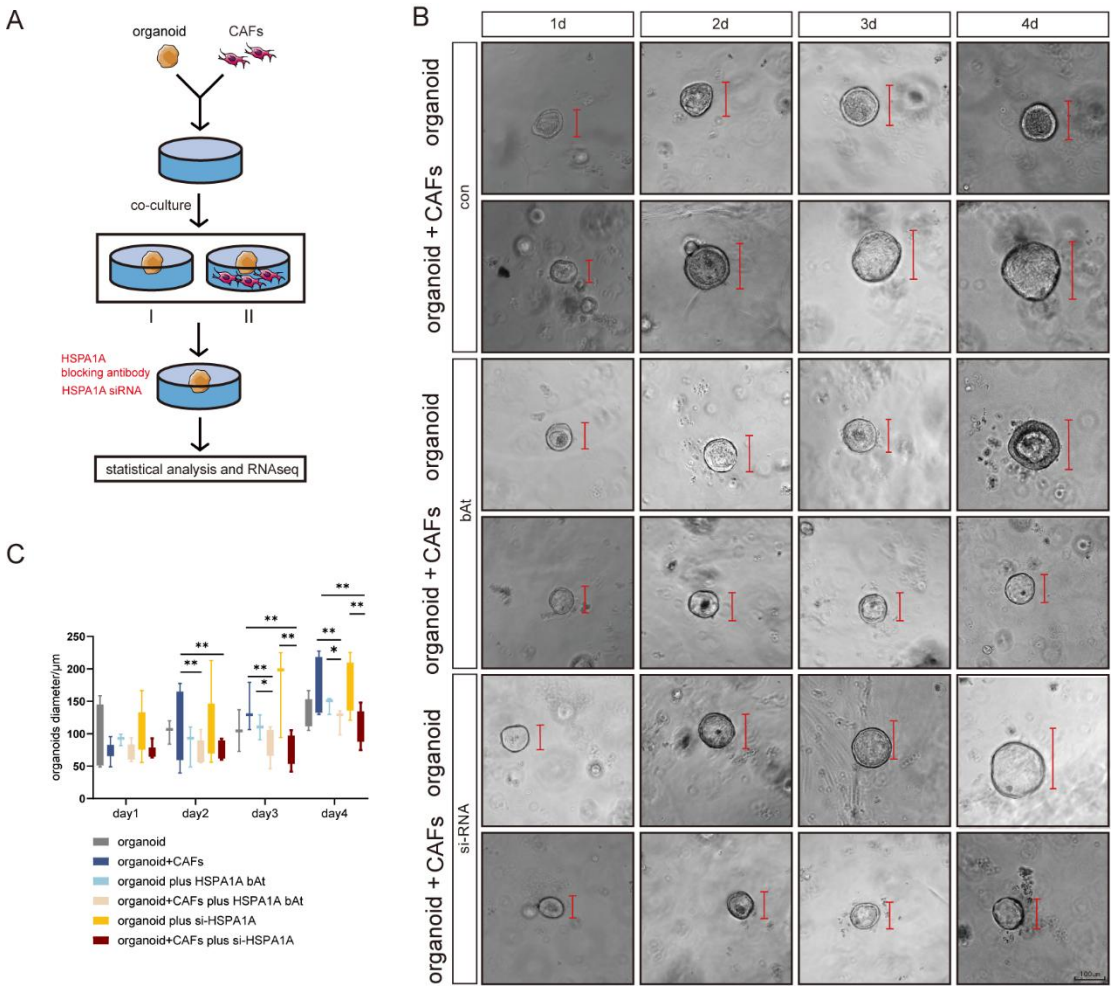

Figure 3. HSPA1A of CAFs promotes the proliferation of GC organoids.

A. Establishment of the co - culture system of GC organoids and CAFs;

B. Representative images of organoids after knocking down HSPA1A in CAFs and adding HSPA1A bAt. Scale bar: 200um

C. Comparison of the diameters of GC organoids in different groups. *P<0.05; **P<0.01.

Collectively, these observations demonstrate that CAF-derived HSPA1A is essential for driving 3D tumor expansion, extending our in vitro findings and reinforcing its role as a key stromal regulator in GC progression.

While CAF-derived HSPA1A markedly enhances GC growth, aggressive tumors are also characterized by poor therapeutic response. We therefore investigated whether this stromal factor contributes not only to tumor expansion but also to reduced treatment efficacy in GC.

CAF-derived HSPA1A selectively enhances the sensitivity of GC organoids to 5-FU and PTX

To assess the clinical relevance of CAF-derived HSPA1A, we tested two commonly used

chemotherapeutic agents for GC, 5-FU and PTX, in the organoid co-culture model. Co-culture with CAFs markedly reduced the growth-inhibitory effect of 5-FU on GC organoids, whereas HSPA1A knockdown in CAFs restored drug sensitivity, resulting in significantly smaller organoid size under 5-FU treatment (**Fig. 4A,C**). Consistently, blockade of extracellular HSPA1A with a neutralizing antibody produced similar effects (**Fig. 4A,C**).

In similar, CAF-derived HSPA1A did significantly alter the antitumor efficacy of PTX, and inhibiting HSPA1A in CAFs reduced the sensitivity of GC organoids to PTX. (**Fig. 4B,D**).

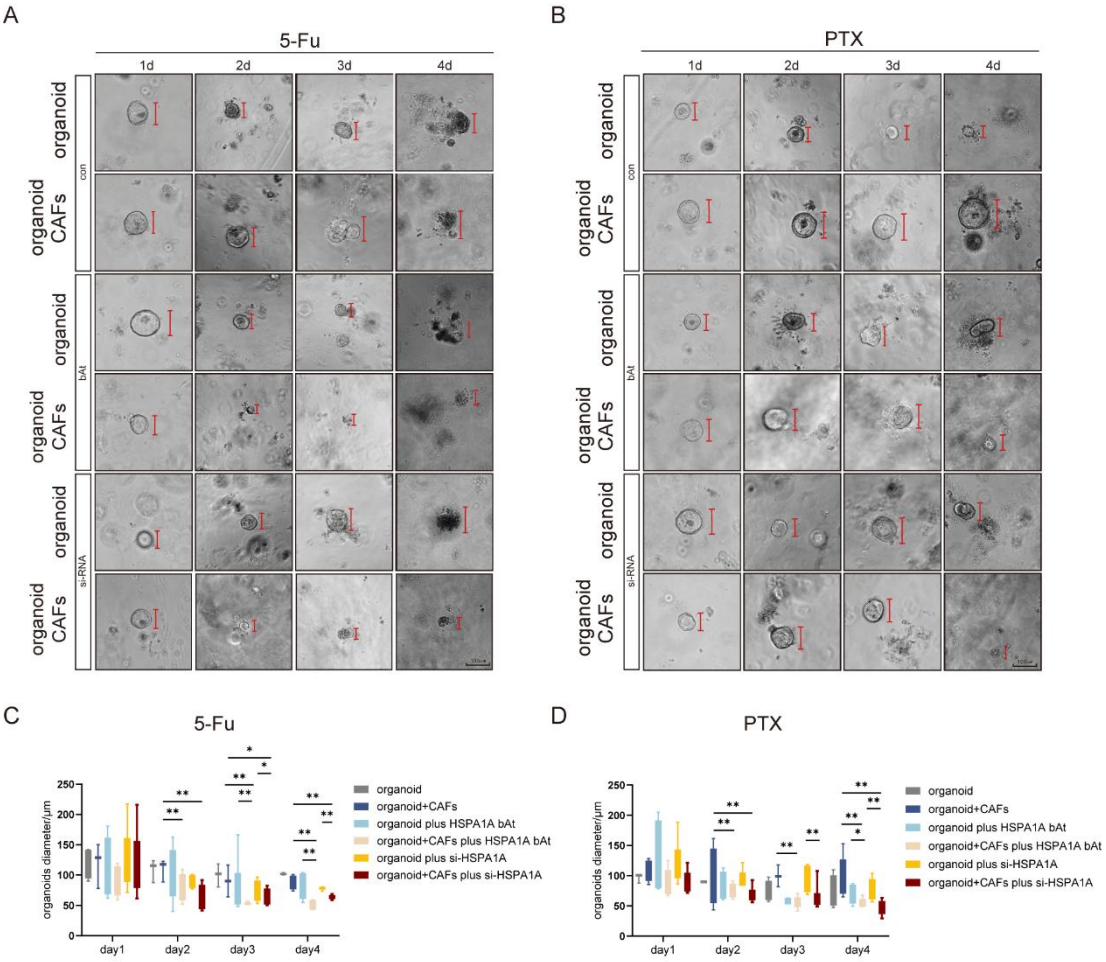

Figure4. Knockdown of HSPA1A in CAFs enhances the sensitivity of GC organoids to chemotherapeutic drugs.

A and C. Under the condition of 5 – FU, graphs and statistical analysis of the diameter changes of organoids in different groups, including organoid, organoid + CAF, organoid + si - HSPA1A, organoid + CAF + si - HSPA1A, organoid + Blocking antibody of HSPA1A , and organoid + CAF + Blocking antibody of HSPA1A;

B and D. Under the condition of PTX, graphs and statistical analysis of the diameter changes of organoids in different groups, including organoid, organoid + CAF, organoid + si - HSPA1A, organoid + CAF + si - HSPA1A, organoid + Blocking antibody of HSPA1A , and

organoid + CAF + Blocking antibody of HSPA1A.
*P<0.05; **P<0.01.

These data indicate that CAF-derived HSPA1A selectively reduces the responsiveness of GC organoids to 5-FU, but has limited influence on PTX-mediated growth inhibition.

Knockdown of CAF-derived HSPA1A suppresses GC growth in vivo

We then asked whether CAF-derived HSPA1A similarly regulates tumor growth and chemosensitivity in vivo and therefore tested its function in a xenograft model. To validate it, a subcutaneous xenograft model was established by injecting AGS cells into nude mice (**Fig. 5A**). When tumors reached ~50 mm^3, mice were randomized to receive intratumoral administration of either control IgG or HSPA1A-blocking antibody, with or without chemotherapy.

Blockade of HSPA1A alone significantly suppressed tumor growth, resulting in decreased tumor volume and weight compared with IgG-treated controls (**Fig. 5B – D**). Moreover, HSPA1A inhibition further enhanced the antitumor effect of 5-FU and PTX, leading to the smallest tumors across all treatment groups (**Fig. 5B–D**), indicating that CAF-derived HSPA1A contributes to reduced chemotherapy efficacy in vivo.

Immunohistochemical staining of harvested tumors showed reduced expression of Ki-67 and PCNA following HSPA1A blockade, both under baseline conditions and in combination with chemotherapy, confirming decreased tumor cell proliferation (**Fig. 5E–F**).

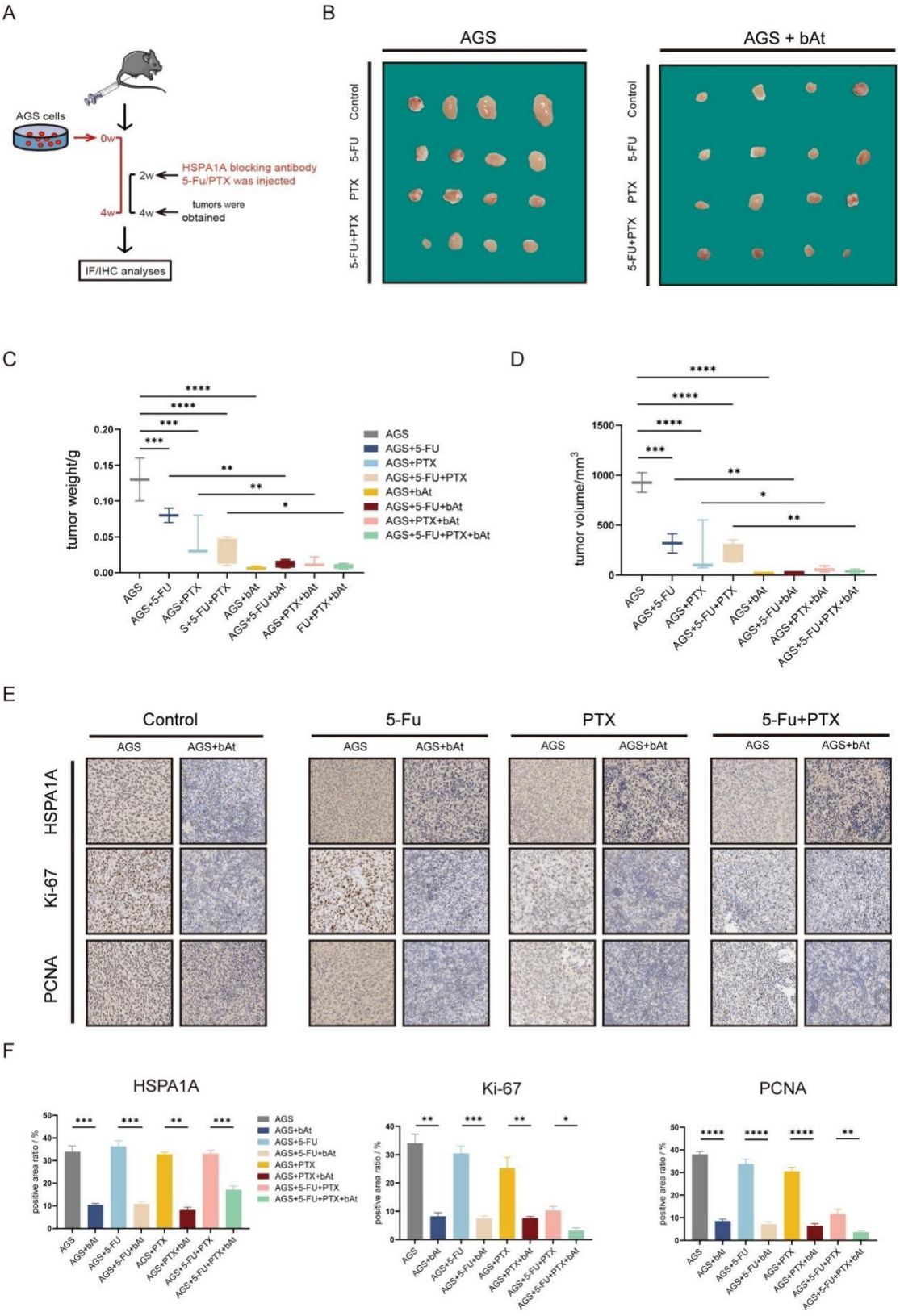

Figure 5. Knockdown of HSPA1A inhibits the growth of GC *in vivo*.

A. Construction of a subcutaneous tumor model in mice;

B. Photos of tumor masses in the HSPA1A bAt group and the control group under normal

conditions and after the addition of 5 - FU and PTX;
C. Statistical analysis of tumor volumes in the HSPA1A bAt group and the control group under normal conditions and after the addition of 5 - FU and PTX;
D. Statistical analysis of tumor weights in the HSPA1A bAt group and the control group under normal conditions and after the addition of 5 - FU and PTX;
E. IHC staining of HSPA1A, Ki - 67, and PCNA in tumor masses of the HSPA1A bAt group and the control group under normal conditions and after the addition of 5 - FU and PTX;
F. Statistical analysis of HSPA1A, Ki - 67, and PCNA positive areas in tumor masses of different groups.
*P<0.05; **P<0.01; ***P<0.001; ****P<0.0001.

These findings demonstrate that CAF-derived HSPA1A is required for robust in vivo tumor growth and dampens the response to chemotherapy.

CAF-derived HSPA1A interacts with SEMG1 to regulate glycolysis in GC cells

To explore the molecular mechanism by which CAF-derived HSPA1A promotes tumor progression, RNA-seq analysis was performed on AGS organoids co-cultured with CAFs versus HSPA1A-silenced CAFs. SEMG1 was significantly downregulated following HSPA1A inhibition in CAFs (**Fig. 6A**), and pathway enrichment analysis revealed suppression of glycolysis-associated signaling (**Fig. 6B**).

Consistent with the transcriptomic data, immunoblotting confirmed that SEMG1 protein levels in AGS cells were reduced when co-cultured with HSPA1A-silenced CAFs, whereas control CAFs maintained higher SEMG1 expression (**Fig. 6C**).

To investigate whether HSPA1A directly interacts with SEMG1, protein–protein docking analysis was performed. Structural modeling predicted a stable HSPA1A–SEMG1 complex with a defined interaction interface (**Fig. 6D**). Detailed analysis of the docking model identified multiple hydrogen bonds between specific residues of HSPA1A and SEMG1, with interaction distances ranging from approximately 2.5 to 3.4 Å, supporting a direct and specific molecular interaction (**Fig. 6E**). This interaction was further validated experimentally by co-immunoprecipitation assays, which demonstrated reciprocal pulldown of HSPA1A and SEMG1 in GC cells (**Fig. 6F**).

Finally, immunofluorescence staining of GC tissues revealed spatial association between HSPA1A-positive stromal regions and SEMG1-positive tumor cells, supporting the physiological relevance of the HSPA1A–SEMG1 axis in vivo (**Fig. 6G**).

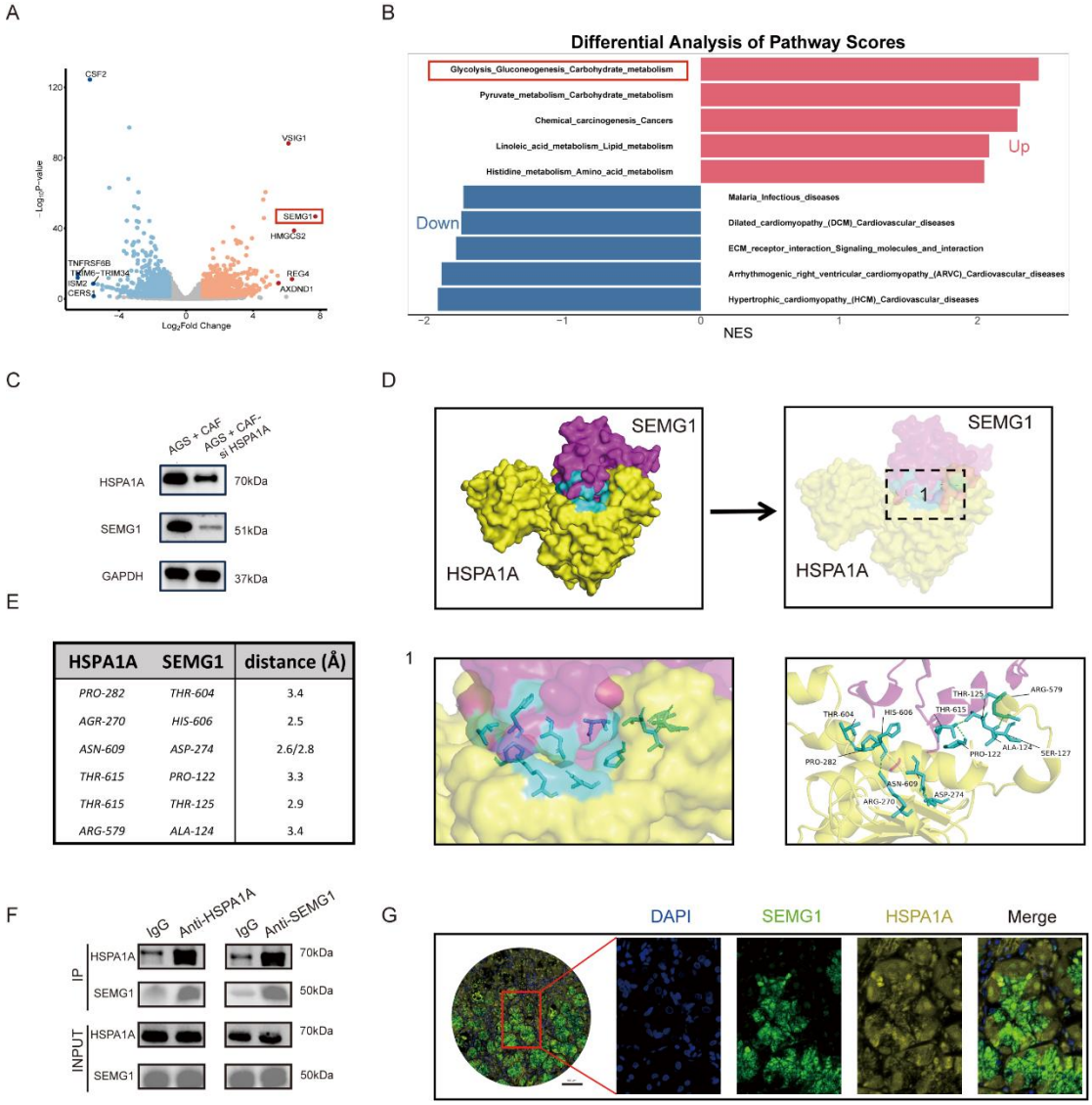

HSPA1A	SEMG1	distance (Å)
PRO-282	*THR-604*	3.4
AGR-270	*HIS-606*	2.5
ASN-609	*ASP-274*	2.6/2.8
THR-615	*PRO-122*	3.3
THR-615	*THR-125*	2.9
ARG-579	*ALA-124*	3.4

Figure 6. CAFs derived HSPA1A affects the glycolysis of GC cells by interacting with SEMG1.

A. A volcano plot presents upregulated and downregulated genes from RNA-seq analysis comparing CAFs plus AGS and si-HSPA1A CAFs plus AGS;

B. Pathway analysis of differentially expressed genes enriched in CAFs and AGS compared to si-HSPA1A CAFs and AGS;

C. Changes of SEMG1 in CAFs co-cultured with AGS AND si-HSPA1A CAFs co-cultured with AGS;

D. The direct interaction between HSPA1A and SMEG1 was analyzed by HDOCK ;

E. Predicted hydrogen bond distances between interacting residues of HSPA1A and SEMG1 based on docking analysis;

F. Co-IP verification of the interaction between HSPA1A and SEMG1;

IF staining of the co-localization of SEMG1 in tumor cells and HSPA1A in CAFs (control group). Scale Bar: 100 μm;

These results indicate that CAF-derived HSPA1A binds to tumor-cell SEMG1 and enhances glycolysis-related signaling, providing a mechanistic explanation for its malignant effects in GC.

Targeting the CAF-HSPA1A–SEMG1 axis suppresses glycolytic flux in GC cells

Given the identification of SEMG1 as a downstream effector of CAF-derived HSPA1A, we next examined whether this axis functionally regulates glycolysis in GC cells. Immunoblot analysis showed that knockdown of SEMG1 in AGS cells led to a marked reduction in the expression of key glycolytic enzymes, including PKM2 and LDHA, whereas the level of G-6-PD was minimally affected (**Fig. 7A**). Similarly, silencing HSPA1A in CAFs reduced PKM2 and LDHA expression in co-cultured AGS cells, and combined inhibition of HSPA1A in CAFs and SEMG1 in tumor cells produced a more pronounced suppression of glycolysis-related proteins (**Fig. 7A**).

Consistently, qRT–PCR analysis revealed coordinated downregulation in the mRNA levels of HSPA1A/SEMG1 and glycolysis-associated genes (PKM2, LDHA, and G6PD) in the corresponding co-culture settings (**Fig. 7B**), supporting transcriptional-level regulation within this axis.

To directly assess glycolytic activity, Seahorse extracellular acidification rate (ECAR) assays were performed. SEMG1 knockdown in AGS cells significantly decreased both basal and compensatory glycolysis compared with control cells (**Fig. 7C–D**). Consistent with these findings, co-culture with control CAFs enhanced glycolytic flux in AGS cells, whereas co-culture with HSPA1A-silenced CAFs markedly attenuated ECAR responses (**Fig. 7E–F**).

Collectively, these results demonstrate that CAF-derived HSPA1A promotes glycolytic reprogramming in GC cells through SEMG1, and that disruption of this stromal–tumor metabolic axis effectively suppresses glycolytic flux (**Fig. 7G**).

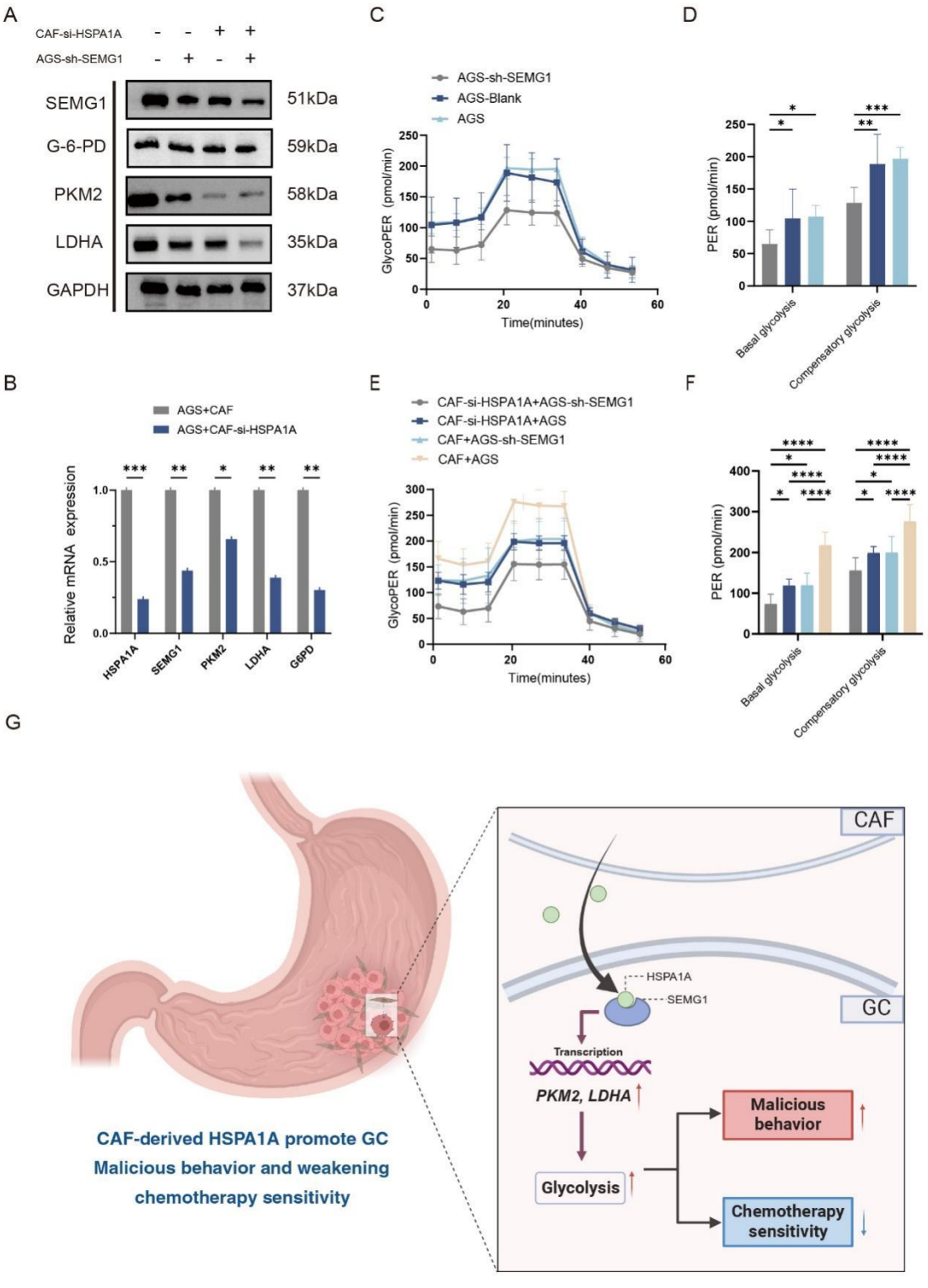

Figure 7. Effect of targeting the HSPA1A-SEMG1 axis on the glycolytic pathway in GC

A. Immunoblot analysis of glycolysis-related enzymes (G-6-PD, PKM2, and LDHA) in AGS cells with SEMG1 knockdown and/or co-cultured with HSPA1A-silenced CAFs;

B. qRT–PCR analysis of HSPA1A, SEMG1, PKM2, LDHA, and G6PD mRNA levels in AGS cells co-cultured with control CAFs or HSPA1A-silenced CAFs (CAF-si-HSPA1A). (n = 5 biological replicates), mean ± SEM.

C and D. Seahorse analysis of basal and compensatory glycolysis in SEMG1-knockdown AGS cells. (n = 8 biological replicates), mean ± SEM.

E and F. Seahorse analysis of glycolytic flux in AGS cells co-cultured with control or HSPA1A-silenced CAFs. (n = 8 biological replicates), mean ± SEM.

These results demonstrate that CAF-derived HSPA1A promotes glycolysis in GC cells through SEMG1.

Discussion

In this study, we identify CAF-derived HSPA1A as a previously unrecognized stromal regulator that promotes GC progression and weakens chemotherapy response. HSPA1A was predominantly expressed in CAFs within tumor tissues and was associated with advanced disease stages and worse prognosis[34][35]. Functionally, CAF-secreted HSPA1A enhanced GC cell proliferation, migration, organoid expansion and tumor growth, demonstrating its essential role in tumor–stroma interactions. More importantly, HSPA1A inhibition sensitized GC cells to 5-FU both in vitro and in vivo, highlighting its therapeutic relevance.

Mechanistically, we demonstrate that CAF-derived HSPA1A exerts its protumorigenic effects through direct interaction with SEMG1 on tumor cells, thereby upregulating glycolytic enzymes (PKM2, LDHA) and sustaining glycolytic flux[24][36]. Silencing either HSPA1A in CAFs or SEMG1 in tumor cells reduced glycolysis, whereas dual inhibition achieved a stronger suppression. These findings support a model in which the HSPA1A–SEMG1 axis enables GC cells to maintain metabolic adaptation in the nutrient-limited tumor microenvironment, ultimately driving aggressive tumor behavior.

Interestingly, HSPA1A inhibition increased sensitivity to 5-FU and PTX, but it seems that the inflence to 5-FU is more obvious. This difference may reflect the distinct cytotoxic mechanisms of these agents: 5-FU targets nucleotide synthesis and preferentially affects highly proliferating and metabolically active cells[37], whereas PTX primarily disrupts microtubule dynamics[38], a process that may be less dependent on glycolytic reprogramming. Therefore, metabolic stress induced by targeting CAF-derived HSPA1A may selectively enhance the efficacy of nucleotide-targeting chemotherapy.

Our findings extend previous studies on HSP70 family proteins in cancer by uncovering a non-cell-autonomous and secretory role for HSPA1A in tumor progression. While tumor-cell-intrinsic HSPA1A has been associated with treatment resistance in several malignancies, our data reveal that stromal HSPA1A is a more pivotal contributor in GC, acting as a paracrine metabolic driver rather than solely a chaperone-mediated survival factor within tumor cells.

There are still limitations to this study. First, although CAF-derived HSPA1A appears to act extracellularly, the specific receptor-like function of SEMG1 and the downstream signaling cascades require further elucidation. Second, only 5-FU andPTX were evaluated; whether CAF-HSPA1A influences responses to targeted therapies or immunotherapy warrants exploration. Finally, our study focused on subcutaneous xenografts, and future work should employ orthotopic or metastatic models to better replicate the gastric tumor microenvironment.

In summary, our work establishes CAF-secreted HSPA1A as a crucial stromal factor that promotes GC progression and improves chemotherapy efficacy by activating SEMG1-dependent glycolysis. Targeting this stromal–tumor metabolic axis may serve as a promising therapeutic strategy to inhibit tumor growth and overcome chemoresistance in GC.

Funding

This study was supported by the National Natural Science Foundation of China (ID 82073023, 82372589, to J. Li; ID 82372821, 82103357 to L.-P. Hu; ID 82002485, to Q. Li), the

independent project of the National Key Laboratory of Tumor System Medicine (ID ZZ-RCPY-25-44, to J. Li), the Shanghai Oriental Talents Program (ID QNWS2025028 to L.-P. Hu), Wu Jie-Ping Medical Foundation (ID WJPJJ242711, to J. Xu), China Health Promotion Foundation (ID zgjkciih242514, to J. Xu).

Author contributions

B.-T.S., W.F., S.-G.H., L.J. and X.J. designed and supervised the overall study, analyzed data, and drafted the manuscript. W.F., S.-G.H., L.R. and W.-T.H. constructed the xenograft model and collected the tissues. B.-T.S., W.F., L.R. and W.-T.H. performed the immunohistochemical staining and analyzed the clinicopathological characteristics and prognosis of gastric cancer. L.H. and Y.-S.Q. technically assisted with experiments and analyzed data. L.Q. and H.-L.P. provided excellent suggestions. C.H. and X.J. provided human gastric cancer tissues. B.-T.S., W.F., S.-G.H., Q.L., H.-L.P., L.J., C.H. and X.J. supervised this study and edited the manuscript.

Competing interests

The authors have declared that no conflict of interest exists.

Reference

[1] Thrift AP, Wenker TN, El-Serag HB. Global burden of gastric cancer: epidemiological trends, risk factors, screening and prevention. Nat Reviews Clin Oncol. 2023;20(5):338–49.

[2] Siegel RL, Miller KD, Jemal A. Cancer statistics, 2018. CA Cancer J Clin. 2018;68:7–30.

[3] Chen W, Zheng R, Baade PD, Zhang S, Zeng H, Bray F, Jemal A, Yu XQ, He J. Cancer statistics in China, 2015. CA Cancer J Clin. 2016;66:115–132.

[4] Allemani C, Matsuda T, Di Carlo V, Harewood R, Matz M, Nikšić M, Bonaventure A, Valkov M, Johnson CJ, Estève J, Ogunbiyi OJ, Azevedo E Silva G, Chen WQ, Eser S, Engholm G, Stiller CA, Monnereau A, Woods RR, Visser O, Lim GH, Aitken J, Weir HK, Coleman MP; CONCORD Working Group. Global surveillance of trends in cancer survival 2000-14 (CONCORD-3): analysis of individual records form 37 513 025 patients diagnosed with one of 18 cancers from 322 population-based registries in 71 countries.

608 Lancet. 2018 Mar 17;391(10125):1023-1075.
609 [5] Van Cutsem E, Sagaert X, Topal B, Haustermans K, Prenen H. Gastric cancer. Lancet. 2016
610 Nov 26;388(10060):2654-2664. doi: 10.1016/S0140-6736(16)30354-3. Epub 2016 May 5.
611 [6] J.A. Ajani, T.A. D'Amico, D.J. Bentrem, J. Chao, D. Cooke, C. Corvera, P. Das, P.C.
612 Enzinger, T. Enzler, P. Fanta, F. Farjah, H. Gerdes, M.K. Gibson, S. Hochwald, W.L.
613 Hofstetter, D.H. Ilson, R.N. Keswani, S. Kim, L.R. Kleinberg, S.J. Klempner, J. Lacy, Q.P.
614 Ly, K.A. Matkowskyj, M. McNamara, M.F. Mulcahy, D. Outlaw, H. Park, K.A. Perry, J.
615 Pimiento, G.A. Poultsides, S. Reznik, R.E. Roses, V.E. Strong, S. Su, H.L. Wang, G.
616 Wiesner, C.G. Willett, D. Yakoub, H. Yoon, N. McMillian, L.A. Pluchino Gastric cancer,
617 version 2.2022, NCCN clinical practice guidelines in oncology J. Natl. Compr. Cancer
618 Netw. : J. Natl. Compr. Cancer Netw., 20 (2) (2022), pp. 167-192
619 [7] de Visser KE, Joyce JA. The evolving tumor microenvironment: From cancer initiation to
620 metastatic outgrowth. Cancer Cell. 2023 Mar 13;41(3):374-403.
621 [8] Xiao Y, Yu D. Tumor microenvironment as a therapeutic target in cancer. Pharmacol Ther.
622 2021 May;221:107753. doi: 10.1016/j.pharmthera.2020.107753. Epub 2020 Nov 28.
623 [9] Liu Y, Li C, Lu Y, Liu C, Yang W. Tumor microenvironment-mediated immune tolerance
624 in development and treatment of gastric cancer. Front Immunol. 2022 Oct 20;13:1016817.
625 [10]Kalluri R. The biology and function of fibroblasts in cancer. Nat Rev Cancer. 2016 Aug
626 23;16(9):582-98.
627 [11]Bhowmick NA, Neilson EG, Moses HL. Stromal fibroblasts in cancer initiation and
628 progression. Nature. 2004 Nov 18;432(7015):332-7.
629 [12]Kobayashi H, Enomoto A, Woods SL, Burt AD, Takahashi M, Worthley DL. Cancer-
630 associated fibroblasts in gastrointestinal cancer. Nat Rev Gastroenterol Hepatol. 2019
631 May;16(5):282-295.
632 [13]Xiao Y, Yu D. Tumor microenvironment as a therapeutic target in cancer. Pharmacol Ther.
633 2021 May;221:107753.
634 [14]Seeneevassen L, Bessède E, Mégraud F, Lehours P, Dubus P, Varon C. Gastric Cancer:
635 Advances in Carcinogenesis Research and New Therapeutic Strategies. Int J Mol Sci. 2021
636 Mar 26 22 (7):3418.
637 [15]Ferretti GDS, Quaas CE, Bertolini I, Zuccotti A, Saatci O, Kashatus JA, Sharmin S, Lu DY,

Poli ANR, Quesnelle AF, Rodriguez-Blanco J, de Cubas AA, Hobbs GA, Liu Q, O'Bryan JP, Salvino JM, Kashatus DF, Sahin O, Barnoud T. HSP70-mediated mitochondrial dynamics and autophagy represent a novel vulnerability in pancreatic cancer. Cell Death Differ. 2024 Jul;31(7):881-896.

[16]Fiengo L, Lauro G, Bellone ML, Bifulco G, Dal Piaz F, De Tommasi N. The plant diterpene epoxysiderol targets Hsp70 in cancer cells, affecting its ATPase activity and reducing its translocation to plasma membrane. Int J Biol Macromol. 2021 Oct 31;189:262-270.

[17]Lei Z, Xia X, He Q, Luo J, Xiong Y, Wang J, Tang H, Guan T, Tian Y, Xu S, Cui S. HSP70 promotes tumor progression by stabilizing Skp2 expression in gastric cancer cells. Mol Carcinog. 2021 Dec;60(12):826-839.

[18]Hartl FU, Hayer-Hartl M. Molecular chaperones in the cytosol: from nascent chain to folded protein. Science. 2002 Mar 8;295(5561):1852-8.

[19]Schmitt E, Gehrmann M, Brunet M, Multhoff G, Garrido C. Intracellular and extracellular functions of heat shock proteins: repercussions in cancer therapy. J Leukoc Biol. 2007 Jan;81(1):15-27.

[20]Shevtsov M, Huile G, Multhoff G. Membrane heat shock protein 70: a theranostic target for cancer therapy. Philos Trans R Soc Lond B Biol Sci. 2018 Jan 19;373(1738):20160526.

[21]Calderwood SK, Khaleque MA, Sawyer DB, Ciocca DR. Heat shock proteins in cancer: chaperones of tumorigenesis. Trends Biochem Sci. 2006 Mar;31(3):164-72.

[22]Zhu L, Ruan J, Zhang Q, Feng L, Deng Y, Dai L, Zheng Y, Feng Z, Xu R, Liu K, Xu N. LDH and glycolytic activity as predictors of immunotherapy response in gastric cancer: a systematic review and meta-analysis. Front Immunol. 2025 Jun 9;16:1605976.

[23]Lehuédé C, Dupuy F, Rabinovitch R, Jones RG, Siegel PM. Metabolic Plasticity as a Determinant of Tumor Growth and Metastasis. Cancer Res. 2016 Sep 15;76(18):5201-8

[24]Shuvalov O, Kizenko A, Petukhov A, Fedorova O, Daks A, Bottrill A, Snezhkina AV, Kudryavtseva AV, Barlev N. SEMG1/2 augment energy metabolism of tumor cells. Cell Death Dis. 2020 Dec 11;11(12):1047.

[25]Canacci AM, Izumi K, Zheng Y, Gordetsky J, Yao JL, Miyamoto H. Expression of semenogelins I and II and its prognostic significance in human prostate cancer. Prostate. 2011 Jul;71(10):1108-14.

[26] L.P. Hu, W. Huang, X. Wang, C. Xu, W.T. Qin, D. Li, G. Tian, Q. Li, Y. Zhou, S. Chen, H.Z. Nie, Y. Hao, J. Song, X.L. Zhang, J. Sundquist, K. Sundquist, J. Li, S.H. Jiang, Z.G. Zhang, J. Ji, Terbinafine prevents colorectal cancer growth by inducing dNTP starvation and reducing immune suppression Mol. Ther. 30(10), 3284–3299 (2022)

[27] Zhou YQ, Bao TS, Xie JX, Yao LL, Yu ST, Li Q, Huang PQ, Zhou WZ, Wang YY, Chen SY, Wang XQ, Zhang XL, Jiang SH, Yi SQ, Zhang ZG, Ma MZ, Hu LP, Xu J, Li J. The SLITRK4-CNPY3 axis promotes liver metastasis of gastric cancer by enhancing the endocytosis and recycling of TrkB in tumour cells. Cell Oncol (Dordr). 2023 Aug;46(4):1049-1067.

[28] Takemura Y, Sekiguchi Y, Syutsubo K, Harada H, Omura T, Li YY, Kubota K. Sequence-Specific Capture of Oligonucleotide Probes (SCOPE): a Simple and Rapid Microbial rRNA Quantification Method Using a Molecular Weight Cutoff Membrane. Appl Environ Microbiol. 2021 Sep 28;87(20):e0116721.

[29] Győrffy B, Surowiak P, Budczies J, Lánczky A. Online survival analysis software to assess the prognostic value of biomarkers using transcriptomic data in non-small-cell lung cancer. PLoS One. 2013 Dec 18;8(12): e82241.

[30] Aiello S, Cassis P, Cassis L, Tomasoni S, Benigni A, Pezzotta A, Cavinato RA, Cugini D, Azzollini N, Mister M, Longaretti L, Thomson AW, Remuzzi G, Noris M. DnIKK2-transfected dendritic cells induce a novel population of inducible nitric oxide synthase-expressing CD4+CD25- cells with tolerogenic properties. Transplantation. 2007 Feb 27;83(4):474-84.

[31] Aberle MR, Burkhart RA, Tiriac H, Olde Damink SWM, Dejong CHC, Tuveson DA, van Dam RM. Patient-derived organoid models help define personalized management of gastrointestinal cancer. Br J Surg. 2018 Jan;105(2):e48-e60.

[32] Zhou X, Zhang H, Jiang Y, Wei L, Chen Y, Zhang J, Gao P, Zhu S, Fang C, Du Y, Su R, He M, Yu J, Wang S, Ding W, Feng L. The role of chemerin in the regulation of cGAS-STING pathway in gestational diabetes mellitus placenta. FASEB J. 2023 Mar;37(3):e22806.

[33] Wik JA, Phung D, Kolan S, Haraldsen G, Skålhegg BS, Hol Fosse J. Inflammatory activation of endothelial cells increases glycolysis and oxygen consumption despite inhibiting cell proliferation. FEBS Open Bio. 2021 Jun;11(6):1719-1730.

[34] Arora N, Alsaied O, Dauer P, Majumder K, Modi S, Giri B, Dudeja V, Banerjee S, Von Hoff

699 D, Saluja A. Downregulation of Sp1 by Minnelide leads to decrease in HSP70 and decrease
700 in tumor burden of gastric cancer. PLoS One. 2017 Feb 13;12(2):e0171827.
701 [35]Ciocca DR, Calderwood SK. Heat shock proteins in cancer: diagnostic, prognostic,
702 predictive, and treatment implications. Cell Stress Chaperones. 2005 Summer;10(2):86-
703 103. doi: 10.1379/csc-99r.1.
704 [36]Hienonen T, Sammalkorpi H, Enholm S, Alhopuro P, Barber TD, Lehtonen R, Nupponen
705 NN, Lehtonen H, Salovaara R, Mecklin JP, Järvinen H, Koistinen R, Arango D, Launonen
706 V, Vogelstein B, Karhu A, Aaltonen LA. Mutations in two short noncoding mononucleotide
707 repeats in most microsatellite-unstable colorectal cancers. Cancer Res. 2005 Jun
708 1;65(11):4607-13.
709 [37]Canöz O, Belenli O, Patiroglu TE. General features of gastric carcinomas and comparison
710 of HSP70 and NK cell immunoreactivity with prognostic factors. Pathol Oncol Res.
711 2002;8(4):262-9.
712 [38]Bhalla KN. Microtubule-targeted anticancer agents and apoptosis. Oncogene. 2003 Dec
713 8;22(56):9075-86.

Supplementary Files

This is a list of supplementary files associated with this preprint. Click to download.

- WesternBlot.docx